Nucleoside Diphosphate Kinase A/*nm*23-H1 Promotes Metastasis of NB69-Derived Human Neuroblastoma

Malin A.E. Almgren,[1,2] K. Cecilia E. Henriksson,[1,2] Jennifer Fujimoto,[3] and Christina L. Chang[1,2]

[1]Department of Medicine, [2]Rebecca and John Moores Cancer Center, and [3]Animal Care Program, University of California at San Diego, La Jolla, California

Abstract

Nucleoside diphosphate kinase A (NDPK-A), encoded by the *nm*23-H1 gene, acts as a metastasis suppressor in certain human tumors such as breast carcinoma. However, evidence also points to NDPK-A functioning as a metastasis promoter in other human tumors including neuroblastoma. In fact, amplification and overexpression of *nm*23-H1 as well as S120G mutation of NDPK-A (NDPK-A^{S120G}) have been detected in 14% to 30% of patients with advanced stages of neuroblastoma. To test whether NDPK-A promotes neuroblastoma metastasis, we established stable transfectants and an orthotopic xenograft animal model from the human neuroblastoma NB69 cell line. We demonstrate that overexpressed NDPK-A or NDPK-A^{S120G} increased both incidence and colonization of neuroblastoma metastasis in animal lungs without significantly affecting primary tumor development. *In vitro*, these metastasis-associated NDPK-A aberrations abrogated retinoic acid-induced neuronal differentiation while increasing cloning efficiency, cell survival, and colony formation of NB69 derivatives. Furthermore, NDPK-A^{S120G} reduced cell adhesion and increased cell migration. Compared with its wild-type, NDPK-A^{S120G} appears more effective in promoting neuroblastoma metastasis. Our results provide the first evidence that NDPK-A behaves as a metastasis promoter at least in human neuroblastoma derived from NB69 cells. The findings not only suggest a prognostic value of NDPK-A in neuroblastoma patients but also caution NDPK-A-targeted treatment for patients with different tumor types. (Mol Cancer Res 2004;2(7):387–94)

Introduction

Tumor metastasis is a complex and dynamic process, involving several cellular events starting with the primary tumor site and ending with new tumor establishment in distal sites. These cellular events include detachment from the primary tumor, local tissue invasion, intravasation, survival in the circulatory system, extravasation, and colonization at target organs. Tumor metastasis remains a major cause of cancer mortality because detection markers and treatment options are currently limited for patients with metastatic tumors.

Nucleoside diphosphate kinase A (NDPK-A) is one of the proteins known to play a role in tumor metastasis. NDPK-A is encoded by the *nm*23-H1 gene and is located at human chromosome 17q21.3 (1-3). Its role in tumor metastasis was initially identified based on its reduced expression in murine melanoma cells with high metastasis potential (2). Subsequent studies have revealed that the expression level of NDPK-A is negatively correlated with the metastatic potential of certain human tumors, including melanoma and breast carcinoma (4), indicating a metastasis-suppressing role of NDPK-A. Transfection and animal studies indeed support the idea that NDPK-A acts as a metastasis suppressor in these types of tumors (4). Intriguingly, a positive correlation between NDPK-A level and metastatic potential has also been observed in other human tumors including neuroblastoma, osteosarcoma, and pancreatic carcinoma (5-9). However, it remains to be determined whether NDPK-A actually acts as a metastasis promoter in these tumor types.

Neuroblastoma arises from the neural crest of the sympathetic nervous system and accounts for 25% of infants and 7% of children with cancers in the United States. Most patients with limited stages (i.e., I and II) of neuroblastoma can be cured by the surgical removal of localized tumors (10, 11). However, the majority of patients with advanced stages (i.e., III and IV) of neuroblastoma die from metastatic disease despite intensive multimodal therapy (12). The gain of the chromosomal segment of 17q21-qter, within which *nm*23-H1 is located, occurs in 54% to 65% of neuroblastoma patients and is associated with poor clinical outcomes (13-15). Amplification and overexpression of *nm*23-H1 have been found in 14% to 30% of advanced neuroblastomas (5, 6, 16). Furthermore, we reported previously a unique point mutation of *nm*23-H1 that results in a Ser120→Gly substitution in NDPK-A (NDPK-A^{S120G}) in 21% of patients with advanced neuroblastomas (17). This mutation appears to be specific for advanced neuroblastoma because it has not been found in patients with limited stages of neuroblastoma or with leukemia or breast carcinoma (17). The association of these NDPK-A aberrations with the high metastatic potential of human neuroblastoma strongly suggests that, in this tumor type, NDPK-A is a metastasis promoter.

The human neuroblastoma NB69 cell line was established from a primary tumor in the adrenal gland (18), where ~50% of human neuroblastomas originate (19). NB69 cells display low invasiveness and no N-*myc* amplification (20), the latter

Received 4/15/04; revised 6/1/04; accepted 6/9/04.
Grant support: NIH RO1 CA78241 and RO1 CA78241S grants (C.L. Chang). The costs of publication of this article were defrayed in part by the payment of page charges. This article must therefore be hereby marked advertisement in accordance with 18 U.S.C. Section 1734 solely to indicate this fact.
Requests for reprints: Christina L. Chang, University of California at San Diego, 4028 Basic Science Building, 9500 Gilman Drive, La Jolla, CA 92093-0688. Phone: 858-822-0307; Fax: 858-822-0301. E-mail: clchang@ucsd.edu

being associated with advanced stages of neuroblastoma (21). For these reasons, we therefore chose the NB69 line as our cell model to examine the role of NDPK-A independent of N-*myc* in neuroblastoma metastasis. We generated stable transfectants from NB69 cells to examine the effects of NDPK-A aberrations, associated with advanced neuroblastomas, on cellular events involved in the metastatic process. We also developed an orthotopic xenograft animal model with severe combined immunodeficient (SCID) mice to determine the incidence and colonization of neuroblastoma metastasis. Our results indicate that NDPK-A acts as a metastasis promoter rather than a metastasis suppressor in human neuroblastoma derived from NB69 cells.

Results

Coexpression of Aberrant NDPK-A and Green Fluorescent Protein by the Human Neuroblastoma NB69 Cell Line

We established from NB69 cells the stNB series of stable transfectants expressing NDPK-A aberrations found in patients with advanced neuroblastomas. The stNB-M and stNB-W transfectants constitutively overexpress NDPK-A^{S120G} and its wild-type, respectively. The vector-transfected stNB-V serves as a negative control. Based on Western blot analysis, all three randomly selected stNB-V clones expressed a very low level of NDPK-A protein (Fig. 1A and B), similar to the parental NB69 cells (data not shown). Compared with stNB-V, we observed a 10 to 25 times greater protein level of ectopic NDPK-A or NDPK-A^{S120G} in randomly selected stNB-W and stNB-M clones, respectively (the ~21 kDa band in Fig. 1A and B). To our surprise, another form of NDPK-A with slower electrophoretic mobility was also detected in stNB-W and stNB-M transfectants with a monoclonal antibody specific for NDPK-A (Fig. 1A and B) but not for the NDPK-B isoform (data not shown). The protein levels of NDPK-A in stNB-W and stNB-M were comparable with 3 to 10 copies of the *nm*23-H1 gene detected in advanced stages of human neuroblastoma (17) as well as a 2- to 20-fold increase in NDPK activity in human tumors (22).

The stNB series coexpress a humanized *Renilla* green fluorescent protein (GFP) from the same transcript of ectopic NDPK-A in a nonfusion form (Fig. 1C), serving as a convenient cell marker (Fig. 1D). All randomly selected clones in the stNB series displayed different GFP intensity based on flow cytometry (data not shown). The stNB-W and stNB-M clones stably coexpressed NDPK-A with GFP in the presence of G418. In addition, this coexpression was faithfully maintained without G418 selection pressure for at least 1 month (data not shown), which is necessary for the *in vivo* studies.

NDPK-A Aberrations Affect Differentiation but not Proliferation of Human Neuroblastoma Cells

Both protein and mRNA levels of NDPK-A are elevated during the S phase of the cell cycle (23), which suggests that a high level of NDPK-A may affect the proliferation rate. As determined by 3-(4,5-dimethylthiazol-2-yl)-2,5-diphenyltetrazolium bromide assay and cell counting, the doubling times of stNB-M, stNB-V, and stNB-W transfectants were 22.9 ± 2.9, 23.6 ± 2.3, and 21.2 ± 1.1 hours, respectively. Thus, NDPK-A overexpression did not significantly affect proliferation of neuroblastoma cells.

Retinoic acid (RA) induces neuroblastoma cells to undergo neuronal differentiation (i.e., neurite extension) while arresting the growth (24). Similar to the parental NB69 cells (25), ~45% of stNB-V transfectants displayed neurite extension when treated with 30 μmol/L all-*trans* RA for 3 days (Fig. 2A). Under the same treatment condition, however, only 1% to 2% of stNB-W and stNB-M displayed neurite extension (Fig. 2A).

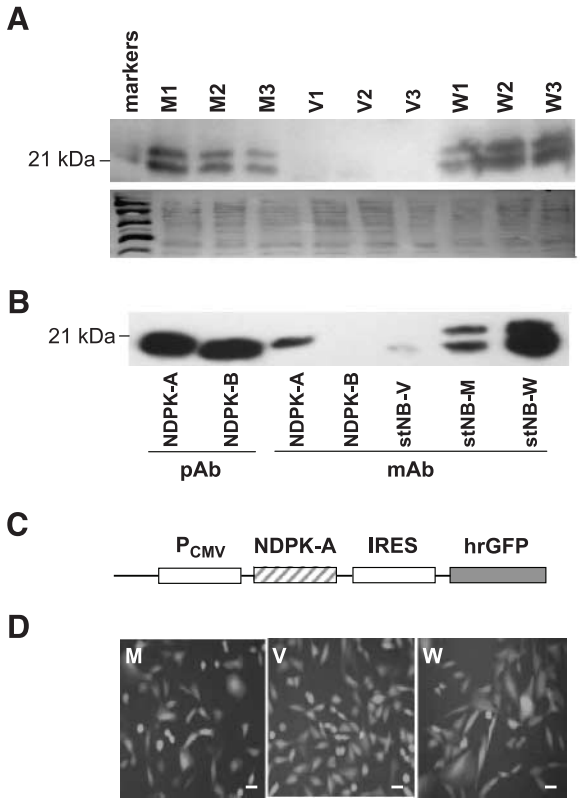

FIGURE 1. Expression of ectopic NDPK-A^{S120G} or its wild-type by fluorescent stable transfectants generated from human neuroblastoma NB69 cells. **A.** Total proteins (50 μg) in cell lysate, prepared from each clone of stNB-M (*M*), stNB-V (*V*), and stNB-W (*W*) transfectants, were resolved by 16% SDS-PAGE and transferred onto a polyvinylidene difluoride membrane. An anti-NDPK-A polyclonal antibody detected ectopic NDPK-A and NDPK-A^{S120G} (apparent molecular mass of ~21 kDa) as well as another protein band with a slow electrophoretic mobility in *W* and *M*, respectively. *Bottom panel,* Coomassie-stained polyacrylamide gel run in parallel with the one above, showing protein amounts being analyzed in each sample. **B.** Western blot analysis of cell lysate of stNB-V, stNB-M, and stNB-W (100 μg total proteins per lysate) using recombinant NDPK-A and NDPK-B (25 ng each, *lanes 1* to *4*) as positive controls. A monoclonal antibody (*mAb*) specific for NDPK-A recognizes both protein bands that were detected with the above-described polyclonal antibody (*pAb*), which cross-reacts with NDPK-B (apparent molecular mass is <21 kDa). **C.** Schematic presentation of a portion of the plasmid construct showing that, under the control of the cytomegalovirus promoter (P_{CMV}), ectopic NDPK-A is coexpressed with a humanized *Renilla* GFP (*hrGFP*) in a nonfusion form from the same transcript via an internal ribosome entry segment (*IRES*). **D.** Photomicrographs of live stNB-M (*M*), stNB-V (*V*), and stNB-W (*W*) transfectants expressing GFP taken under an inverted fluorescent microscope. Scale bars, 40 μm.

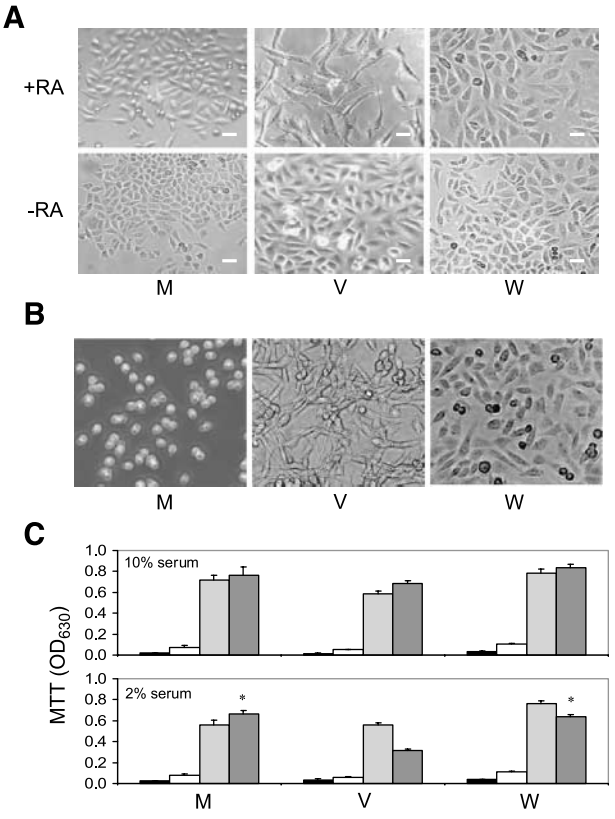

FIGURE 2. Effects of overexpressed NDPK-A or NDPK-A^{S120G} on neuronal differentiation, adhesion, and serum-independent survival of human neuroblastoma cells. **A.** NDPK-A aberrations abrogated the neuronal differentiation and growth arrest of neuroblastoma cells induced by RA. The stNB-M (*M*), stNB-V (*V*), and stNB-W (*W*) transfectants were treated with (*+RA*) or without (*-RA*) 30 μmol/L all-*trans* RA for 3 days, and photomicrographs were taken. Neuronal differentiation is scored when the neurite exceeds one cell body diameter in length. Cell numbers were manually counted. Scale bars, 40 μm. **B.** NDPK-A^{S120G} reduced the adhesion of *M* transfectants, which remained in rounded shape without spreading, compared with *V* and *W* transfectants when plated in the bacterial culture dish for at least 5 days. In addition, the *V* transfectants displayed neurite extension. **C.** NDPK-A aberrations increased the survival of *M* and *W* transfectants when the serum level in growth medium was reduced from 10% (*upper panel*) to 2% (*bottom panel*) after 8 days of culturing without medium replenishment. *, $P < 0.0001$, both versus V (*t* test). The cell number resulting from proliferation and death was examined by 3-(4,5-dimethylthiazol-2-yl)-2,5-diphenyltetrazolium bromide assay after culturing for 1 (*black bar*), 2 (*white bar*), 5 (*light gray bar*), and 8 (*dark gray bar*) days. All data are representative of three independent experiments.

Concomitant with neurite extension, RA inhibited stNB-V growth, whereas stNB-W and stNB-M escaped RA-induced growth arrest and accumulated cell numbers similar to the untreated counterparts (Fig. 2A). These results indicate that overexpression of NDPK-A or NDPK-A^{S120G} abrogates RA-induced neuronal differentiation and maintains neuroblastoma cells in a proliferating state.

The S120G Mutation of NDPK-A Decreases Adhesion of Neuroblastoma Cells

Decreased cell adhesion is associated with the metastatic phenotype of tumors. Relative to stNB-W and stNB-V, we consistently observed that stNB-M transfectants displayed a subtle difference in cell adhesion. At 20% or 95% cell confluency, stNB-M transfectants took 20% to 30% less time than stNB-V or stNB-W transfectants to detach from mammalian cell culture dishes when treated with 0.25% trypsin. Mammalian cells adhere and grow well on the hydrophilic surface of tissue culture dishes and plates. The surface of bacterial culture dishes is relatively more hydrophobic, which might manifest the subtle difference observed in stNB-M adhesion. Indeed, we found that whereas stNB-W and stNB-V attached and spread onto bacterial Petri dishes within 2 days after plating, stNB-M remained rounded without spreading on the dish surface for at least 5 days (Fig. 2B). Rounded stNB-M cells were viable based on trypan blue exclusion (data not shown). In addition, stNB-V, but not stNB-W or stNB-M, displayed neurite extension 4 to 5 days after plating in Petri dishes (Fig. 2B), which further supports our earlier observation that NDPK-A aberrations abrogated neuronal differentiation.

NDPK-A Aberrations Increase Survival and Cloning Efficiency of Neuroblastoma Cells

To metastasize effectively to distal organs, tumor cells must improve their survival ability and cloning efficiency. We first examined whether NDPK-A affects serum-independent survival of neuroblastoma cells. The stNB series of transfectants were cultured at two different serum levels for 8 days without medium replenishment, and cell survival was determined by the 3-(4,5-dimethylthiazol-2-yl)-2,5-diphenyltetrazolium bromide assay on days 1, 2, 5, and 8. Compared with cells in the growth medium containing 10% serum, 90%, 46%, and 74% of stNB-M, stNB-V, and stNB-W, respectively, survived in medium containing 2% serum on day 8 (Fig. 2C). To determine the cloning efficiency, cells were singly sorted by flow cytometry into 96-well plates, three plates per transfection type. The cloning efficiency was calculated as 32 ± 3.2%, 26 ± 2.2%, and 15 ± 1.2% for stNB-W, stNB-M, and stNB-V, respectively. Taken together, our results indicate that NDPK-A aberrations significantly increased cloning efficiency ($P < 0.02$, *t* test) and serum-independent cell survival ($P < 0.0001$, *t* test) of human neuroblastoma cells by 1.6- to 2-fold.

NDPK-A Aberrations Affect In vitro Migration and Colonization of Neuroblastoma Cells

Migration is essential for invading tumor cells to translocate from the primary tumor site to distal organs. Using a modified Boyden chamber system, GFP-labeled stNB-M, stNB-V, and stNB-W were allowed to migrate toward 5% serum in 15 hours. Migrated cells attached underneath the chamber membrane were detected with an inverted fluorescent microscope. After normalizing with the plating cell density, migrated stNB-M and stNB-W cells were 2.2- and 1.3-fold higher than migrated stNB-V, respectively (Fig. 3A), indicating that NDPK-A^{S120G} significantly ($P \leq 0.05$, *t* test) enhanced neuroblastoma cell migration.

We further investigated whether NDPK-A aberrations affect neuroblastoma colonization on soft agar. Transfectants were resuspended in 0.3% agar before being overlaid onto 0.5% agar containing the growth medium. Colonies consisting of at least 50 cells were counted 14 days after plating. The stNB-M and

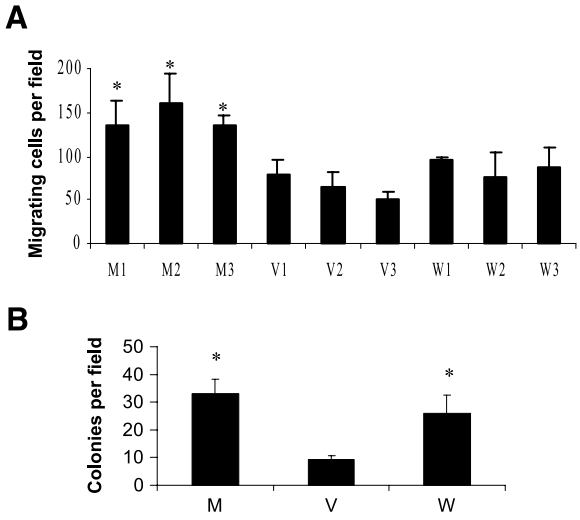

FIGURE 3. Effects of overexpressed NDPK-A or NDPK-A^{S120G} on migration and colony formation of human neuroblastoma cells. **A.** NDPK-A^{S120G} increased the ability of stNB-M (*M*) transfectants, relative to stNB-V (*V*), to migrate toward 5% serum within 15 hours in a modified Boyden chamber system. Migrated cells were photographed at three different and random fields per membrane under a fluorescent microscope with 100× magnification. *Columns,* average migrating cells per field from at least three independent experiments after normalization with the cell density; *bars,* SD. *, $P \leq 0.05$, all versus *V2*, a representative *V* clone (*t* test). **B.** NDPK-A aberrations improved soft agar colonization of the *M* and stNB-W (*W*) transfectants. Colonies were photographed at four different fields under a light microscope with 40× magnification after cells were plated for 14 days. Colonies consisting of ≥50 cells were counted. *Columns,* average colonies per field from three independent experiments; *bars,* SD. *, $P \leq 0.0007$, both versus *V* (*t* test).

stNB-W cells exhibited 3.6- and 2.8-fold more colonies on soft agar, respectively, than stNB-V (Fig. 3B), indicating that NDPK-A aberrations provide neuroblastoma cells with additional *in vitro* colonization ability ($P \leq 0.0007$, *t* test).

NDPK-A Aberrations Do Not Affect Primary Neuroblastoma Development in an Orthotopic Animal Model

The NB69 cell line was established from an adrenal neuroblastoma of a young patient (18). We therefore performed an intraadrenal (i.e., orthotopic) injection of the stNB-M, stNB-V, or stNB-W clones in SCID mice 7 to 8 weeks old using eight mice per clone. All animals developed the primary tumors near the injection site, which were visible as early as 6 days after injection with the tumor reaching ~5 mm in diameter 14 to 18 days after injection. The primary tumor was allowed to grow ~15 mm in diameter or until the animals showed discomfort, which ever occurred first, corresponding to 28 ± 2.5, 24 ± 0.6, or 23 ± 2.3 days after injection with stNB-M, stNB-V, or stNB-W, respectively (Table 1). During necropsy, the primary tumor was found exclusively in the injected adrenal gland (i.e., left) and extended to the left kidney in all mice examined. The average size of primary tumors derived from stNB-M, stNB-V, and stNB-W was 11 ± 1.7, 13 ± 1.7, and 12 ± 1.7 mm in diameter, respectively (Table 1). The latency and size of primary tumors in all animals did not differ significantly among the stNB-V, stNB-M, and stNB-W transfectants. This suggests that NDPK-A does not play a role in primary neuroblastoma development.

NDPK-A Aberrations Increase the Incidence and Colonization of Neuroblastoma in Animal Lungs

When the adrenal neuroblastoma was removed to establish the NB69 cell line, the patient displayed no detectable metastases. At the time of death despite 11 months of radiation and chemotherapy, however, the primary neuroblastoma had metastasized to the lung, liver, and sternum (18). We focused on the lung metastasis to avoid potential spillover into the abdominal cavity during intraadrenal injection. Macroscopic metastases were readily detectable in animal lungs by monitoring the GFP-labeled transfectants without microscopy (Fig. 4A).

Table 1. Overexpression of NDPK-A or NDPK-A^{S120G} Increases the Incidence of Lung Metastasis in an Orthotopic Xenograft Animal Model of Human Neuroblastoma

	M1	M2	M3	V1	V2	V3	W1	W2	W3
Total no. injected mice per clone	8	8	8	8	8	8	8	8	7*
Age ± SD, d	50 ± 2	56 ± 2	51 ± 4	49 ± 2	50 ± 3	56 ± 2	49 ± 3	54 ± 2	54 ± 2
Tumor growth time ± SD, d	26 ± 2	31 ± 1	28 ± 1	24 ± 2	25 ± 2	24 ± 1	24 ± 2	20 ± 2	24 ± 1
Primary tumor size ± SD, mm†	12 ± 2	9 ± 2	12 ± 3	12 ± 3	15 ± 1	12 ± 2	13 ± 3	13 ± 2	10 ± 3
No. mice with macrometastasis	4	4	3	2	1	2	3	1	4
No. mice with macrometastases and micrometastases	4	6	7	3	2	2	5	2	6
Incidence of lung metastasis	M = 17/24‡ (71%)			V = 7/24 (29%)			W = 11/23§ (48%)		

NOTE: Derived from the human neuroblastoma NB69 cell line, three different clones of stNB-M (M1, M2, and M3) and stNB-W (W1, W2, and W3) transfectants overexpress NDPK-A^{S120G} and NDPK-A, respectively. These six clones and three clones of vector-transfected control cells, stNB-V (V1, V2, and V3), were separately injected into the left adrenal gland of SCID mice. During necropsy, the diameters of the primary tumors were measured and averaged and SD was calculated. Macroscopic lung metastasis was readily detectable based on GFP-positive tumor using the naked eye and a fluorescent imaging system. Microscopic metastasis, with at least 10 cells per tumor focus, was determined under a light microscope for animal lung sections stained with H&E. Number of mice with macrometastasis is defined as the number of animals that displayed at least one fluorescent tumor nodule per animal lungs. Number of mice with macrometastases and micrometastases is defined as the number of animals that displayed at least one fluorescent tumor nodule or one tumor focus per animal lungs. Incidence of lung metastasis is expressed as the total number of mice that displayed macrometastases and/or micrometastasis after injecting 24 mice with three clones of M, V, or W, and the corresponding percentage is shown in parentheses. Age is expressed in days at the time when animals were injected with neuroblastoma cells. Tumor growth time is defined as the number of days between injection and necropsy dates.
*Eight mice were injected, but one died with no collectable information.
† Tumor size is measured in diameter.
‡ $P < 0.004$ versus the V clones (Fisher's exact test).
§ $P = 0.04$ versus the V clones (Fisher's exact test).

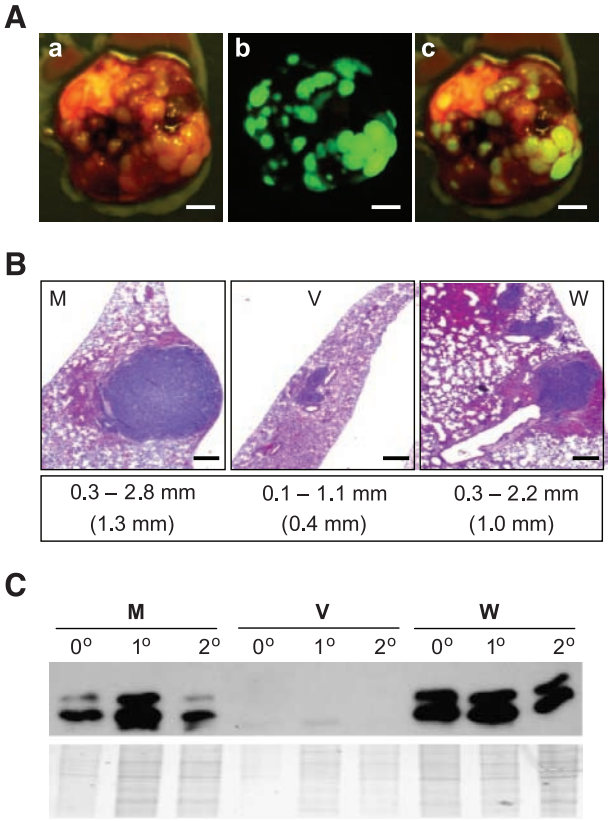

FIGURE 4. Overexpressed NDPK-A or NDPKA^{S120G} promotes metastatic colonization of human neuroblastoma in animal lungs. **A.** Photographs of macroscopic lung metastases of a SCID mouse injected with stNB-M transfectants taken under polarized light (*a*), fluorescent light showing GFP-expressing neuroblastoma (*b*), and both polarized and fluorescent light (*c*). Scale bars, 3 mm. **B.** Photomicrographs of neuroblastoma foci (*dark purple*) in animal lung sections stained with H&E and representative tumor foci in animal lungs after injection with stNB-M (*M*), stNB-V (*V*), and stNB-W (*W*) transfectants. Scale bars, 0.25 mm. Measuring only the largest tumor focus from the lung of each animal, the size distributions and averages of tumor foci in the 72 mice injected with *M*, *V*, and *W* (from left to right) were calculated (*lower panel*). **C.** Western blot analysis of ectopic NDPK-A and NDPKA^{S120G} in the original lines (*0°*) of *M*, *V*, and *W* used for injection and in the cell lines reestablished from the primary (*1°*) and secondary (*2°*) neuroblastomas developed in animals. *Bottom panel,* Coomassie-stained gel run in parallel showing the amount of proteins being analyzed in each sample.

Macroscopic lung metastases (i.e., one or more fluorescent tumor nodules on the lungs) were found in 11, 5, and 8 of the animals injected with stNB-M, stNB-V, and stNB-W, respectively (Table 1). With light microscopy, microscopic lung metastases (i.e., one of more tumor foci containing at least 10 cells per cluster on the lungs) were detected in six, two, and five additional animals injected with stNB-M, stNB-V, and stNB-W respectively (Table 1). By adding the number of animals with macroscopic or microscopic metastases, the incidence was 71%, 29%, and 56% for animals injected with stNB-M, stNB-V, and stNB-W, respectively. Compared with stNB-V, stNB-M ($P < 0.004$) and stNB-W ($P = 0.04$) significantly promoted neuroblastoma metastasis in SCID mice based on Fisher's exact test.

Tumor growth at the secondary site (i.e., metastatic colonization) is a key regulatory step in metastasis. We therefore further examined the effect of NDPK-A aberrations on the ability of the stNB series of transfectants to proliferate and colonize in animal lungs. Counting directly from the fluorescent images taken from only one side of lungs, such as Fig. 4A, three animals injected with stNB-M, one with stNB-W, and none with stNB-V displayed 15 to 40 tumor nodules per mouse lung. The rest of animals with lung metastasis displayed 1 to 10 tumor nodules, and nodule sizes were predominantly larger in animals injected with stNB-M or stNB-W than that with stNB-V. Measuring only the largest microscopic tumor focus in the lungs of each animal, size distributions of tumor foci derived from stNB-M, stNB-V, and stNB-W were 0.3 to 2.8 mm (1.3 mm on average), 0.1 to 1.1 mm (0.4 mm on average), and 0.3 to 2.2 mm (1.0 mm on average) in diameter, respectively (Fig. 4B). These findings indicate that a high level of NDPK-A or NDPK-A^{S120G} promotes metastatic colonization of human neuroblastoma in animal lungs.

NDPK-A and GFP Are Stably Coexpressed in Primary and Metastatic Neuroblastomas in SCID Mice

By G418 selection in culture, we reestablished cell lines from the primary and secondary tumor foci in animals injected with stNB-M, stNB-V, and stNB-W. We found that 100% of the cells in reestablished lines expressed GFP, as detected by fluorescent microscopy (data not shown). Based on Western blot analysis, protein levels of NDPK-A or NDPK-A^{S120G} in the reestablished cell lines were similar to that in the stNB series of transfectants used for animal injection (Fig. 4C). The findings indicate that ectopic NDPK-A was stably maintained and coexpressed with GFP during tumorigenesis and metastasis in our animal model of human neuroblastoma, supporting the role of NDPK-A in neuroblastoma metastasis.

Discussion

In this study, we provide the first evidence that NDPK-A behaves as a metastasis promoter in human neuroblastoma at least in neuroblastoma derived from NB69 cells. This metastasis-promoting role of NDPK-A in neuroblastoma is independent of cell proliferation and primary tumor development, similar to the metastasis-suppressing role of NDPK-A in other tumor types (4). The dual role of a protein in tumor metastasis is not unprecedented because CD44 also plays opposite roles in the metastasis of neuroblastoma and breast carcinoma (26). Neuroblastoma is derived from the neural crest, which is destined to migrate and differentiate during embryonic development. NDPK-A expression is high in early development and decreases with advanced gestational age in the human placenta (27). It is plausible that different genetic backgrounds between embryonic tumors (e.g., neuroblastoma) and non-embryonic tumors (e.g., breast carcinoma) may allow NDPK-A to play different roles in metastasis. Alternatively, genetic alterations may accumulate differently among tumor types and/or between low invasive (e.g., neuroblastoma NB69) and high invasive (e.g., breast cancer MDA-MB435) cells (4) used in studying the role of NDPK-A in metastasis. Similarly, we cannot rule out that certain genetic alterations unique to NB69 and not occurring in other human neuroblastoma cell lines may cooperate with NDPK-A in promoting the metastasis. It is also likely that NDPK-A acts as a metastasis promoter in

neuroblastoma because of the presence of an additional form of NDPK-A, which displays a slow electrophoretic mobility. This variant form may be a post-translationally modified NDPK-A, or *nm*23-H1B, a splice variant of NDPK-A that contains 25 additional residues at the NH_2 terminus (28). We are currently investigating the nature of this variant form of NDPK-A.

The metastasis-suppressing role of NDPK-A has been correlated with its motility-inhibitory effect on human breast cancer and murine melanoma cells (29, 30). In human neuroblastoma NB69 cells, however, NDPK-A did not exhibit any motility/migration-suppressing effect. In fact, NDPK-A^{S120G} significantly enhanced the migration of neuroblastoma cells by ~2-fold. Similarly, the S120G mutation of NDPK-A also allows breast cancer cells to become more mobile by abrogating its motility-inhibitory effect (29). The S120G mutation of NDPK-A may increase cell motility/migration by reducing its phosphotransferase activity (31, 32) and/or the two-component kinase-like activity (33). Alternatively, the S120G mutation may increase cell motility/migration by altering its protein folding and protein-protein interactions (31, 34).

Tiam1 is one of proteins that interact with NDPK-A (35). NDPK-A inhibits Tiam1 activity specific for Rac1 and therefore may affect Rac1-mediated actin polymerization and lamellipodia formation, which are essential for cell adhesion and migration (35-37). Interestingly, NDPK-A protein has been detected in lamellipodia of human fibroblasts (38), which is likely due to an indirect interaction with integrin cytoplasmic domain-associated protein-1α via NDPK-B (1, 38) and/or via Tiam1 and Rac1 (39). It is known that integrin cytoplasmic domain-associated protein-1α associates with the cytoplasmic domain of β_1 integrin (40), and the latter is up-regulated by overexpression of DR-*nm*23 (another member of the NDPK family) in human SK-N-SH and murine N1E-115 neuroblastoma cells (41). It would be interesting to investigate whether Tiam1 and/or integrins are involved in increased migration and reduced adhesion of NB69 cells expressing NDPK-A^{S120G}.

RA induces neuronal differentiation and the growth arrest of neuroblastoma cells (24) and has been used for treating neuroblastoma patients (42). Neuroblastoma cells containing N-*myc* amplification have been shown to develop resistance to RA (43). NB69 cells display no N-*myc* amplification (18, 20) and undergo growth arrest and neuronal differentiation in responding to RA (25). However, overexpression of NDPK-A, either wild-type or S120G mutant, abrogated the effect of RA on NB69 cells. This abrogation may be due to the activity of certain interacting proteins altered by NDPK-A aberrations, such as Tiam1 and Rad (44). It is known that overexpression of Tiam1 or Rad stimulates cell spreading and neurite extension in the murine neuroblastoma N1E-115 cells (45, 46). Interestingly, NDPK-A overexpression in combination with N-*myc* amplification in human neuroblastoma IMR-32 cells enhances neuronal differentiation in the presence or absence of RA (47). When considering RA treatment, and until the regulation of neuronal differentiation is fully understood, it is important to determine whether neuroblastoma patients display NDPK-A aberrations and/or N-*myc* amplification because these genetic alterations have occurred individually or in combination (5, 6, 17).

In conclusion, NDPK-A does not behave as a metastasis suppressor in human neuroblastoma derived from NB69 cells. Overexpression and S120G mutation of NDPK-A promote neuroblastoma metastasis not only by preventing neuronal differentiation but also by increasing cell survival and colonization. Additionally, NDPK-A^{S120G} is able to reduce cell adhesion while increasing migration, rendering it a more potent metastasis promoter than its wild-type. Our findings suggest that NDPK-A is a potential marker for predicting the clinical outcome of neuroblastoma patients and the effectiveness of treatment with RA. Our findings also expand the role of NDPK-A from a metastasis suppressor to a metastasis promoter in certain tumor types, cautioning NDPK-A-based diagnostic and therapeutic development.

Materials and Methods

Expression Plasmids and Stable Transfectants

Using previously described pCRII-*nm*23H1-wt and pCRII-*nm*23H1-mut plasmids as templates (31), the respective cDNAs were amplified with a pair of primers: A-70 (GTT GGA TCC CAG CTG GAA GGA ACC ATG GC) and A-494 (GGT TCT CGA GCA TGG GAA GGA GGG GAA ATG G). The PCR products were cloned into the pIRES-hrGFP-1a vector (Stratagene, La Jolla, CA) followed by an insertion of the Neo-resistant gene via the pExchange module EC-Neo (Stratagene). The resulting expression plasmids were confirmed by DNA sequencing in the Cancer Center Core Facility of the University of California at San Diego (La Jolla, CA).

The human neuroblastoma NB69 cell line (18), generously provided by Dr. Jorge A. Colombo (Programa Unidad de Neurobiologia Aplicada, PRUNA, CEMIC-CONICET, Argentina), was cultured in DMEM-F12 medium (Invitrogen, Carlsbad, CA) containing 10% (v/v) fetal bovine serum (Invitrogen) at 37°C in a humidified atmosphere of 6% CO_2. Using the Effectene reagents (Qiagen, Valencia, CA), NB69 cells (2×10^5 per well, six-well plates) were transfected with the above-described expression plasmids (1 μg) mixed with 8 μL Effectene enhancer and 10 μL Effectene reagent according to the manufacturer's instruction. Stable transfectants were selected with 400 μg/mL G418 before being cloned by Flow Cytometry at the Cancer Center Core Facility of University of California at San Diego.

Proliferation and Differentiation of Neuroblastoma Cells

To determine the proliferation rate, transfectants were plated at 2×10^4 cells/mL in 6- or 96-well plates in triplicates for 1 week and fed every other day. Cell numbers in each well of the six-well plates were measured daily by a Coulter Counter (model Z, Beckman Coulter, Inc., Fullerton, CA) and plotted against hours to determine the doubling time during exponential growth. The proliferation rate was confirmed with a modified 3-(4,5-dimethylthiazol-2-yl)-2,5-diphenyltetrazolium bromide assay in 96-well plates using a standard curve for cell numbers. At least three independent experiments were performed.

To induce neuronal differentiation, neuroblastoma cells were seeded at 1×10^4 cells/mL in 24-well plates and treated in the dark with 30 μmol/L all-*trans* RA (Sigma Chemical Co., St. Louis, MO), whereas the negative control was treated with

the vehicle (i.e., ethanol). Three days after treatment, cells at three different and random locations per well were photographed with a CCD camera attached to an inverted microscope (Leica Microsystems, Inc., Bannockburn, IL, model DMIRB). Cells were scored positive for neuronal differentiation if neurites exceeded one cell body diameter in length. To determine the effect of RA on cell arrest, cells from different fields of microphotographs were manually counted and averaged for each treatment condition. Different treatment conditions were duplicated in each of three independent experiments.

Western Blot Analysis

The total proteins (50 to 100 μg) extracted from each clone of transfectants were resolved by 16% SDS-PAGE blotted onto the polyvinylidene difluoride membrane as described previously (31). NDPK-A on the membrane was probed with 1 μg/mL anti-NDPK-A monoclonal antibody (Kamiya Biomedical Co., Seattle, WA) or 0.67 μg/mL anti-NDPK-A polyclonal antibody (Santa Cruz Biotechnology, Santa Cruz, CA) followed by a horseradish peroxidase–conjugated secondary antibody and chemiluminescence as described previously (31). To confirm the specificity of antibodies, recombinant NDPK-A and NDPK-B were generated as described previously (31).

Cell Migration Assay

Exponentially growing cells (2.5×10^4 in 500 μL) in the DMEM-F12 medium containing 0.1% serum were added to a modified Boyden chamber in duplicates. Subsequently, each chamber containing cells was placed into a well of 24-well plates containing 500 μL DMEM-F12 medium supplemented with 5% serum, which serves as the source of chemoattractants. Cells were allowed to migrate toward 5% serum through the FluroBloc membrane (BD Biosciences, Lexington, KY) for 15 hours at 37°C and 6% CO_2. The FluroBloc membrane blocks 99% of fluorescence from nonmigrating cells; therefore, migrated GFP-expressing transfectants attached underneath the membrane were directly photographed in three different and random fields under an inverted fluorescent microscope (100× magnification). At least three independent experiments were performed.

Colony Formation on Soft Agar

Exponentially growing cells were resuspended in 0.3% agar, at a density of 2×10^4 cells/mL, before being overlaid onto 0.5% agar in a well of six-well plates in duplicates. Once the agar solidified, cells were fed with the growth medium twice a week for 2 weeks. Under a light microscope with 40× magnification, photographs were taken at four different and random fields per well. At least three independent experiments were performed.

Intraadrenal Injection

Six-week-old female Fox Chase SCID mice (Charles River Laboratories, Wilmington, MA) were maintained in a pathogen-free environment for at least 1 week prior to experimentation. Before surgery, the SCID mice were anesthetized with 75 mg/kg ketamine (Fort Dodge Animal Health, Fort Dodge, IA) and 1 mg/kg medetomidine (Pfizer Animal Health, Exton, PA) i.p. Additional anaesthetic was given when necessary. An incision was made over the left retroperitoneal space exposing the left adrenal gland into which 0.6×10^6 neuroblastoma cells in 10 μL PBS were injected with a disposable 30 G needle attached to a 25 μL syringe (Hamilton, Reno, NV). The incision was closed with 4-0 dexon, and each animal was given 0.5 mL saline and 0.1 mg/kg buprenorphine (Rickitt and Coleman Pharmaceuticals Inc., Richmond, VA) s.c. During the first week after surgery, animals were given sulfamethoxazole trimethoprim antibiotics in the drinking water. Animal studies were preformed in accordance with protocols approved by the Animal Subjects Committee of the University of California at San Diego.

Detection of Macroscopic and Microscopic Neuroblastoma Metastases in SCID Mice

After intraadrenal injection, the general health of animals and tumor development were monitored daily for the first week followed by three times per week. Animals were sacrificed when tumors reached ~1.5 cm in diameter when the animals showed a high level of discomfort or 1 month after injection, whichever came first. Animal lungs were examined and photographed under polarized and/or fluorescent light for macroscopic metastases with an imaging system consisting of an Epi lighting system with 470 nm excitation, 515 nm emission filters, a CCD camera (Illumatool Model LT-9500, Lightools Research, Encinitas, CA), and MagnaFire SP imaging software version 2.1 (Optronics, Goleta, CA). Microscopic metastases were examined by light microscopy in lung tissues after they had been fixed, paraffin embedded, serial sectioned, and stained with H&E.

Reestablishment of Cell Lines from Primary and Metastatic Human Neuroblastomas in an Orthotopic Xenograft Animal Model

Human neuroblastomas, ~3 mm in diameter, were excised from the primary and secondary tumor foci in SCID mice. Excised tumors were washed in sterile PBS containing 50 units/mL penicillin and 50 μg/mL streptomycin, and tumor cells were dispersed by needles. Human neuroblastoma cells resistant to G418 were selected from animal cells by culturing with growth medium containing 400 μg/mL G418 at 37°C and 6% CO_2 for 10 to 14 days.

Statistical Analyses

A two-tailed Student's t test was used to compare the mean values of cell survival, migration, or soft agar colonization between the control (stNB-V) and the transfectants that overexpress NDPK-A variants (i.e., stNB-W and stNB-M). Fisher's exact test was used to compare the incidence of lung metastasis between SCID mice injected with stNB-V and those with stNB-M or stNB-W. In both tests, $P \leq 0.05$ was considered significant.

Acknowledgments

We thank Jorge A. Colombo for the kind gift of the NB69 cell line; Yamei Cheng, Jin Il Kim, Ralph Thurlow, and Kay Bates for their technical assistance; and Gordon Gill, Deching Chang, and Larry Paris for suggestions and critical reading of the manuscript.

References

1. Gilles AM, Presecan E, Vonica A, et al. Nucleoside diphosphate kinase from human erythrocytes. Structural characterization of the two polypeptide chains responsible for heterogeneity of the hexameric enzyme. J Biol Chem 1991;266: 8784-9.

2. Steeg PS, Bevilacqua G, Kopper L, Thorgeirsson UP, Talmadge JE, Liotta LA, et al. Evidence for a novel gene associated with low tumor metastatic potential. J Natl Cancer Inst 1988;80:200-4.

3. Backer JM, Mendola CE, Kovesdi I, et al. Chromosomal localization and nucleoside diphosphate kinase activity of human metastasis-suppressor genes *NM*23-1 and *NM*23-2. Oncogene 1993;8:497-502.

4. Hartsough MT, Steeg PS. *Nm*23/nucleoside diphosphate kinase in human cancers. J Bioenerg Biomembr 2000;32:301-8.

5. Leone A, Seeger RC, Hong CM, et al. Evidence for *nm*23 RNA overexpression, DNA amplification and mutation in aggressive childhood neuroblastomas. Oncogene 1993;8:855-65.

6. Hailat N, Keim DR, Melhem RF, et al. High levels of p19/*nm*23 protein in neuroblastoma are associated with advanced stage disease and with N-*myc* gene amplification. J Clin Invest 1991;88:341-5.

7. Oda Y, Naka T, Takeshita M, et al. Comparison of histological changes and changes in *nm*23 and c-MET expression between primary and metastatic sites in osteosarcoma: a clinicopathologic and immunohistochemical study. Hum Pathol 2000;31:709-16.

8. Nakamori S, Ishikawa O, Ohhigashi H, et al. Expression of nucleoside diphosphate kinase/*nm*23 gene product in human pancreatic cancer: an association with lymph node metastasis and tumor invasion. Clin Exp Metastasis 1993;11:151-8.

9. Nakamori S, Ishikawa O, Ohigashi H, et al. Clinicopathological features and prognostic significance of nucleoside diphosphate kinase/*nm*23 gene product in human pancreatic exocrine neoplasms. Int J Pancreatol 1993;14:125-33.

10. Alvarado CS, London WB, Look AT, et al. Natural history and biology of stage A neuroblastoma: a Pediatric Oncology Group study. J Pediatr Hematol Oncol 2000;22:197-205.

11. Perez CA, Matthay KK, Atkinson JB, et al. Biologic variables in the outcome of stages I and II neuroblastoma treated with surgery as primary therapy: a Children's Cancer Group study. J Clin Oncol 2000;18:18-26.

12. Matthay KK, Villablanca JG, Seeger RC, et al. Treatment of high-risk neuroblastoma with intensive chemotherapy, radiotherapy, autologous bone marrow transplantation, and 13-*cis*-retinoic acid. Children's Cancer Group. N Engl J Med 1999;341:1165-73.

13. Lastowska M, Van Roy N, Bown N, et al. Molecular cytogenetic delineation of 17q translocation breakpoints in neuroblastoma cell lines. Genes Chromosomes Cancer 1998;23:116-22.

14. Abel F, Ejeskar K, Kogner P, et al. Gain of chromosome arm 17q is associated with unfavorable prognosis in neuroblastoma, but does not involve mutations in the somatostatin receptor 2 (SSTR2) gene at 17q24. Br J Cancer 1999;81:1402-9.

15. Bown N, Cotterill S, Lastowska M, et al. Gain of chromosome arm 17q and adverse outcome in patients with neuroblastoma. N Engl J Med 1999;340:1954-61.

16. Takeda O, Handa M, Uehara T, et al. An increased *NM*23H1 copy number may be a poor prognostic factor independent of LOH on 1p in neuroblastomas. Br J Cancer 1996;74:1620-6.

17. Chang CL, Zhu XX, Thoraval DH, et al. *Nm*23-H1 mutation in neuroblastoma. Nature 1994;370:335-6.

18. Feder MK, Gilbert F. Clonal evolution in a human neuroblastoma. J Natl Cancer Inst 1983;70:1051-6.

19. Brodeur GM, Sawada T, Tsuchida Y, et al. Neuroblastoma. Amsterdam: Elsevier Science B.V.; 2000.

20. Zaizen Y, Taniguchi S, Suita S. The role of cellular motility in the invasion of human neuroblastoma cells with or without N-*myc* amplification and expression. J Pediatr Surg 1998;33:1765-70.

21. Brodeur GM, Seeger RC, Schwab M, et al. Amplification of N-*myc* in untreated human neuroblastomas correlates with advanced disease stage. Science 1984;224:1121-4.

22. Lacombe ML, Sastre-Garau X, Lascu I, et al. Overexpression of nucleoside diphosphate kinase (*Nm*23) in solid tumors. Eur J Cancer 1991;27:1302-7.

23. Keim D, Hailat N, Melhem R, et al. Proliferation-related expression of p19/*nm*23 nucleoside diphosphate kinase. J Clin Invest 1992;89:919-24.

24. Giannini G, Dawson MI, Zhang X, et al. Activation of three distinct RXR/RAR heterodimers induces growth arrest and differentiation of neuroblastoma cells. J Biol Chem 1997;272:26693-701.

25. Mena MA, Casarejos MJ, Estrada C, et al. Effects of retinoic acid on NB 69 human neuroblastoma cells and fetal rat mid brain neurons. J Neural Transm Park Dis Dement Sect 1994;8:85-97.

26. Kauffman EC, Robinson VL, Stadler WM, et al. Metastasis suppression: the evolving role of metastasis suppressor genes for regulating cancer cell growth at the secondary site. J Urol 2003;169:1122-33.

27. Okamoto T, Iwase K, Niu R. Expression and localization of *nm*23-H1 in the human placenta. Arch Gynecol Obstet 2002;266:1-4.

28. Ni X, Gu S, Dai J, et al. Isolation and characterization of a novel human *NM*23-H1B gene, a different transcript of *NM*23-H1. J Hum Genet 2003;48:96-100.

29. MacDonald NJ, Freije JMP, Stracke ML, et al. Site-directed mutagenesis of *nm*23-H1. Mutation of proline 96 or serine 120 abrogates its motility inhibitory activity upon transfection into human breast carcinoma cells. J Biol Chem 1996; 271:25107-16.

30. Kantor JD, McCormick B, Steeg PS, et al. Inhibition of cell motility after *nm*23 transfection of human and murine tumor cells. Cancer Res 1993;53: 1971-3.

31. Chang CL, Strahler JR, Thoraval DH, et al. A nucleoside diphosphate kinase A (*nm*23-H1) serine 12→glycine substitution in advanced stage neuroblastoma affects enzyme stability and alters protein-protein interaction. Oncogene 1996; 12:659-67.

32. Freije JM, Blay P, MacDonald NJ, et al. Site-directed mutation of *Nm*23-H1. Mutations lacking motility suppressive capacity upon transfection are deficient in histidine-dependent protein phosphotransferase pathways *in vitro.* J Biol Chem 1997;272:5525-32.

33. Wagner PD, Steeg PS, Vu ND. Two-component kinase-like activity of *nm*23 correlates with its motility-suppressing activity. Proc Natl Acad Sci USA 1997; 94:9000-5.

34. Lascu I, Schaertl S, Wang C, et al. A point mutation of human nucleoside diphosphate kinase A found in aggressive neuroblastoma affects protein folding. J Biol Chem 1997;272:15599-602.

35. Otsuki Y, Tanaka M, Yoshii S, et al. Tumor metastasis suppressor *nm*23H1 regulates Rac1 GTPase by interaction with Tiam1. Proc Natl Acad Sci USA 2001; 98:4385-90.

36. Habets GG, Scholtes EH, Zuydgeest D, et al. Identification of an invasion-inducing gene, Tiam-1, that encodes a protein with homology to GDP-GTP exchangers for Rho-like proteins. Cell 1994;77:537-49.

37. Raftopoulou M, Hall A. Cell migration: Rho GTPases lead the way. Dev Biol 2004;265:23-32.

38. Fournier HN, Dupe-Manet S, Bouvard D, et al. Integrin cytoplasmic domain-associated protein 1α (ICAP-1α) interacts directly with the metastasis suppressxsor *nm*23-H2, and both proteins are targeted to newly formed cell adhesion sites upon integrin engagement. J Biol Chem 2002;277:20895-902.

39. Degani S, Balzac F, Brancaccio M, et al. The integrin cytoplasmic domain-associated protein ICAP-1 binds and regulates Rho family GTPases during cell spreading. J Cell Biol 2002;156:377-87.

40. Chang DD, Wong C, Smith H, et al. ICAP-1, a novel β1 integrin cytoplasmic domain-associated protein, binds to a conserved and functionally important NPXY sequence motif of β1 integrin. J Cell Biol 1997;138: 1149-57.

41. Amendola R, Martinez R, Negroni A, et al. DR-*nm*23 gene expression in neuroblastoma cells: relationship to integrin expression, adhesion characteristics, and differentiation. J Natl Cancer Inst 1997;89:1300-10.

42. Reynolds CP, Lemons RS. Retinoid therapy of childhood cancer. Hematol Oncol Clin North Am 2001;15:867-910.

43. Peverali FA, Orioli D, Tonon L, et al. Retinoic acid-induced growth arrest and differentiation of neuroblastoma cells are counteracted by N-*myc* and enhanced by max overexpressions. Oncogene 1996;12:457-62.

44. Zhu J, Tseng YH, Kantor JD, et al. Interaction of the ras-related protein associated with diabetes rad and the putative tumor metastasis suppressor *NM*23 provides a novel mechanism of GTPase regulation. Proc Natl Acad Sci USA 1999;96:14911-8.

45. Leeuwen FN, Kain HE, Kammen RA, et al. The guanine nucleotide exchange factor Tiam1 affects neuronal morphology; opposing roles for the small GTPases Rac and Rho. J Cell Biol 1997;139:797-807.

46. Ward Y, Yap SF, Ravichandran V, et al. The GTP binding proteins Gem and Rad are negative regulators of the Rho-Rho kinase pathway. J Cell Biol 2002; 157:291-302.

47. Backer MV, Kamel N, Sandoval C, et al. Overexpression of *NM*23-1 enhances responsiveness of IMR-32 human neuroblastoma cells to differentiation stimuli. Anticancer Res 2000;20:1743-9.